Available online at www.sciencedirect.com
SCIENCE DIRECT®
Biochimica et Biophysica Acta xx (2005) xxx–xxx
BIOCHIMICA ET BIOPHYSICA ACTA
BBA
http://www.elsevier.com/locate/bba

High pressure reveals that the stability of interdimeric contacts in the R- and T-state of HbA is influenced by allosteric effectors: Insights from computational simulations

I. Kövesi [a], G. Schay [a], T. Yonetani [b], M. Laberge [a,b], J. Fidy [a,*]

[a] *Department of Biophysics and Radiation Biology and MTA Biophysics Research Group, Semmelweis University, Budapest, H-1088 Puskin utca 9, Hungary*
[b] *Department of Biochemistry and Biophysics, Johnson Research Foundation, University of Pennsylvania, Philadelphia, PA 19104-6059, USA*

Received 16 September 2005; received in revised form 6 December 2005; accepted 6 December 2005

Abstract

The molecular details of the mechanism of action of allosteric effectors on hemoglobin oxygen affinity are not clearly understood. The global allostery model proposed by Yonetani et al. suggests that the binding of allosteric effectors can take place both in the R and T states and that they influence oxygen affinity through inducing global tertiary changes in the subunits. Recently published high pressure studies yielded dissociation constants at atmospheric pressure that showed a stabilizing effect of heterotropic allosteric effectors on the dimer interface in the R state, and a more pronounced destabilizing effect in a T state model. In the present work, we report on computational modeling used to interpret the high pressure experimental data. We show structural changes in the hemoglobin interdimeric interfaces, indicative of a global tertiary structural change induced by the binding of allosteric effectors. We also show that the number of water molecules bound at the interface is significantly influenced by binding effectors in the T state in accordance with the experimental data. Our results suggest that the binding of effectors at definite sites leads to tertiary changes that propagate to the interfaces and results in overall structural re-organizations.

Keywords: Human hemoglobin; Hb allostery; Heterotropic effector; MD simulation; Dimer interface; High pressure

1. Introduction

Tetrameric human hemoglobin (Hb) consists of two dimers, $\alpha_1\beta_1$ and $\alpha_2\beta_2$—and the close contact regions of two subunits within each $\alpha\beta$ dimer are referred to as the intradimeric interfaces, namely the $\alpha_1\beta_1$ and $\alpha_2\beta_2$ interfaces. Four additional interdimeric interfaces mediate contact in the tetramer: $\alpha_1\beta_2$, $\alpha_2\beta_1$, $\alpha_1\alpha_2$, and $\beta_1\beta_2$. The quaternary transition that Hb undergoes as it shuttles between oxygenated and deoxygenated states was described as a change in the relative orientations of the $\alpha_1\beta_1$ and $\alpha_2\beta_2$ dimers- and of the intra/interdimeric interfaces, as soon as three-dimensional structures became available for both states [1]. Thus, the interfaces can be used as prime indicators of both tertiary and quaternary changes.

Recently, we reported the results of a high pressure study investigating the effect of heterotropic effectors on the tetramer–dimer equilibria of human adult hemoglobin (Hb) [2]. We compared oxyHb (R-state) to a well-known T-state analog, α-oxyFe-βZn-Hb. High pressure resulted in a red shift of the Trp fluorescence emission accompanied by a significant increase of the quantum yield. We interpreted the phenomenon as pressure-induced dimerization, fitting the data to a simple dissociation model. Taking into account the pressure dependence of the dissociation constant, we were able to fit the data to a theoretical curve that yielded the dissociation constant for the tetramer–dimer transition at atmospheric pressure. The results showed that allosteric effectors destabilized the T-state tetramer but stabilized the R-state. The magnitude of the effect was also consistent with IHP being a more potent effector than DPG [3].

In this work, we use a molecular dynamics (MD) approach to interpret our experimental findings. We build up Hb models for

Abbreviations: Hb, human hemoglobin A; IHP, inositol hexaphosphate; oxyHb, oxygenated Hb; α-oxyFe-β-ZnHb, (α Fe-O_2)$_2$-(β zinc-protoporphyrin-IX)$_2$; DPG, 2,3-diphosphoglycerate

* Corresponding author. Fax: +36 1 2666656.
E-mail address: judit@puskin.sote.hu (J. Fidy).

1570-9639/$ - see front matter © 2005 Elsevier B.V. All rights reserved.
doi:10.1016/j.bbapap.2005.12.002

the conditions used in the experiments, namely: stripped Hb, and Hb in the presence of Cl^- ions or DPG for both quaternary states and subject all models to 2 ns of MD simulations at constant pressure and temperature (CPT). Full details of the MD simulations will be reported elsewhere. In this report, we only characterize the interdimeric interfaces and describe how the presence of effectors modifies their structural properties. The results support the recently proposed global allostery model [4,5] that reformulates the classical models by proposing that effector-linked tertiary changes modulate the oxygen affinity of Hb rather than the quaternary transition associated with oxygen binding at the heme.

2. Materials and methods

Preparation of the initial Hb models from RCSB repository coordinates (R-state Hb, T-state Hb, T-state Hb+DPG) and from a docking study(R-state Hb+DPG) is fully described elsewhere, as well as the 500-ps molecular dynamics protocol, which was extended to 2 ns [6]. Briefly, all simulations were performed using CHARMM version c31b2 with the all-atom 27 protein forcefield included in the distribution [7] and with NAMD2 [8]. Explicit hydrogens were added using HBUILD consistent with pH 7.0. All models were explicitly solvated in equilibrated TIP3P water boxes under periodic boundary conditions in boxes of approximately the same size. For example, the R-state Hb system consisted of 63155 explicit atoms in a box of size 90 Å×81 Å×81 Å, i.e., 582 protein residues and 18,029 water molecules. Counterions were added to maintain charge neutrality in all models, and to reflect physiological salt concentrations (0.154 mol/l)—except for the stripped models. To model the chloride binding sites in the Hb-chloride models, Cl^- ions were placed in the central cavity close to α-Val1 and where DPG binds [9]. After heating and equilibration MD, 2 ns-production trajectories were acquired and the average structure calculated. CPT simulations were performed (P=0.1 MPa, T=300 K) as previously described [6,10]. All simulations yielded stable conformational states with backbone rmsd deviations not exceeding ~1.2 Å. After simulations, interface residues were identified as those residues whose SASA decreases by more than 1 $Å^2$ after forming the interface. The properties of these residues were calculated using SURFNET [11] or extracted from the simulated structures using routine CHARMM analysis scripts. These properties include the following: (a) the interface gap volume: to calculate it, each pair of subunit atoms are considered in turn, inserting a sphere (max r=5 Å) halfway between the surfaces of the two atoms, such that the sphere surface makes contact with the surfaces of both atoms in the pair. If any other atoms intercept this sphere, the size of the sphere is accordingly reduced. When the size of the sphere falls below a minimum (r=1 Å), the sphere is discarded. When the sphere remains after this procedure, its size is recorded. The sizes of all the allowable gap-spheres are then used to calculate the gap volume between the two subunits; (b) solvent accessible surface areas (SASA) were calculated using the Connolly algorithm [12] with a probe sphere of radius of 1.4 Å. Interfaces were further analyzed for hydrophobic interactions using the MolSurfer program, a graphical tool that links a 2D projection of a macromolecular interface to a 3D view of the macromolecular structures [13]. The program calculates hydrophobicities assigned according to the Eisenberg scale [14].

3. Results

Fig. 1 shows the shape of the overall interdimeric interface ($\alpha_1\beta_2+\alpha_2\beta_1+\alpha_1\alpha_2+\beta_1\beta_2$) extracted from the 2 ns-average MD structures. The notable difference in interface extent between the R and T states is of course expected, but we also note significant shape differences as a result of effector binding, much more pronounced in the R state. Table 1 lists the parameters calculated for specific interfaces properties, namely the number of residues making up the interface, the number of bridging water molecules

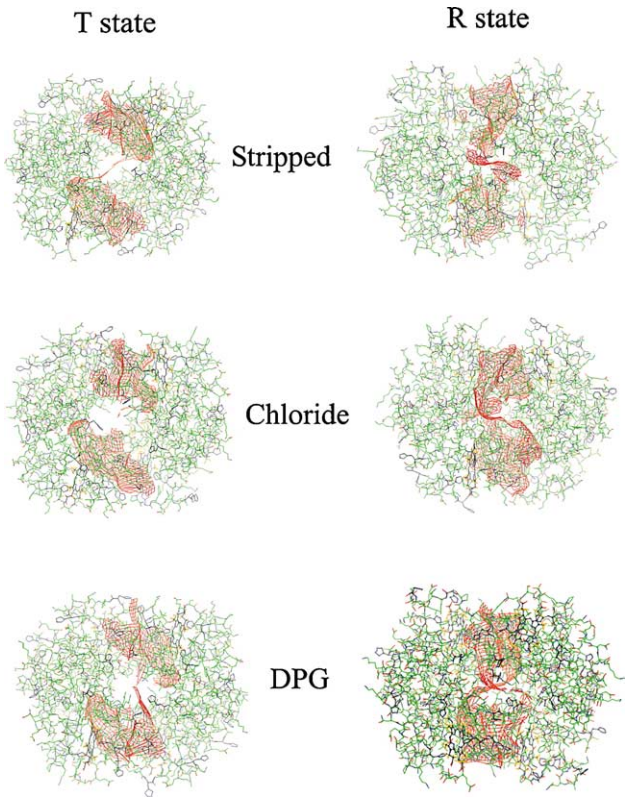

Fig. 1. MolSurfer screen snapshots of the sum of the interdimeric interface regions (red mesh) in the various Hb R and T states.

present, the total number of waters present, the number of hydrogen bonds, the SASA, and the interface gap volume. To evaluate the meaning of these quantities, we primarily considered the values characterizing the whole interface, that is, those shown in the last column. As for the contribution of the individual interfaces, the $\beta_1\beta_2$ interface may play a role in the case of DPG binding—as will be discussed later.

Of interest is to note that the $\alpha_1\beta_2$ and $\alpha_1\beta_2$ interface properties differ from each other. This is due to an inherent asymmetry in the HbA αβ dimers, already noticeable when superimposing the respective dimer coordinates of the starting X-ray structures that yield a backbone rmsd of 0.23 Å between dimers. In the present study, we focus our attention on the characteristics of the whole interdimeric interfaces, and assume that they are correctly represented in the model obtained after 2 ns dynamics. As shown below, the agreement with experimental data support the validity of our approach. Table 1 shows that, besides the expected differences between R and T state Hb, the presence of chloride or DPG affects all parameters to a significant extent. Fig. 2 shows that the bridging waters in the $\alpha_1\beta_2$ T-state interface are affected by the presence of Cl^- (bottom) and DPG (middle). The bridging waters – as well as the H-bond network – having a different distribution among the different interface regions when Hb is bound to effectors are associated with a complex reorganization of the interface contacts, with new residues becoming part of an interface, and others no longer included. In this work, we analyze the interfaces obtained from the MD models to support the experimental data

Table 1
Structural parameters of the interdimeric interface region of the average structures obtained after 2 ns MD simulations for R and T state Hb models

	R state interfaces					
	α1β2	α2β1	α1α2	β1β2	All	Values/ residue
Stripped						
Interface residues	26	18	22	15	81	
Bridging waters	8	2	5	4	19	0.23
Total waters	33	30	22	35	120	1.48
H-bonds	1	1	1	3	6	0.07
Gap volume [Å^3]	3917.1	4543.1	4659.8	5557.9	18,677.9	230.59
SASA [Å^2]	897.9	481.1	670	578.1	2627.1	32.43
Cl						
Interface residues	25	23	23	17	88	
Bridging waters	7	9	3	4	23	0.26
Total waters	30	25	28	35	118	1.34
H-bonds	4	1	7	0	12	0.14
Gap volume [Å^3]	4105.7	4706.4	5470.4	5668.7	19,951.2	226.72
SASA [Å^2]	992.8	851.7	908.2	404	3156.7	35.87
DPG						
Interface residues	24	25	21	9	79	
Bridging waters	5	3	3	3	14	0.18
Total waters	19	33	41	25	118	1.49
H-bonds	5	4	5	0	14	0.18
Gap volume [Å^3]	3551.7	3785	5126.3	5447.1	17,910.1	226.71
SASA [Å^2]	1008.2	924.6	732.2	130.6	2795.6	35.39
	T state interfaces					
	α1β2	α2β1	α1α2	β1β2	All	Values/ residue
Stripped						
Interface residues	28	26	19	–	73	
Bridging waters	5	6	6	–	17	0.23
Total waters	19	24	22	–	65	0.89
H-bonds	2	1	6	–	9	0.12
Gap volume [Å^3]	3265.9	3720.1	4543.1	–	11,529.1	157.93
SASA [Å^2]	1140.6	1070	607.5	–	2818.1	38.6
Cl						
Interface residues	28	24	14	–	66	
Bridging waters	2	6	4	–	12	0.18
Total waters	31	38	20	–	89	1.35
H-bonds	5	1	4	–	10	0.15
Gap volume [Å^3]	3610	4531.5	4776.4	–	12,917.9	195.73
SASA [Å^2]	1162.6	917.7	499	–	2579.3	39.08
DPG						
Interface residues	29	27	12	6	74	
Bridging waters	7	4	1	4	16	0.22
Total waters	27	19	55	29	130	1.76
H-bonds	2	2	5	0	9	0.12
Gap volume [Å^3]	5103	3563.4	4274.9	5837.8	18,779.1	253.77
SASA [Å^2]	1084.2	1020.6	562.6	115	2782.4	37.6

on the dimerization K_d values. Thus, we do not analyze the reorganization of the interfaces in full details.

3.1. The R-state interfaces

For R state HbA, we do not have an experimental K_d value for DPG, only for Cl^- and IHP, known to be a stronger effector. Both effectors decreased the K_d; Cl^- had a slight effect, IHP decreased it by a factor of 3. In the simulation data, the effect of chloride and DPG seems to be different, but in both cases, the net effect is that they act in the direction of stronger binding. The number of interface residues is almost unchanged with DPG, but significantly increased with chloride. It seems reasonable that the SASA is thus increased with Cl^- while remaining almost unchanged with DPG. The gap volume is slightly increased with Cl^-, not as much as would be expected considering the larger size of the interface. With DPG, the volume is smaller, more than expected from the slight decrease in the number of residues. With Cl^-, the number of bridging waters increases while with DPG, the number decreases by the same amount. The number of interface H-bonds is increased significantly, by a factor of 2 with Cl^- and by a factor of 2.6 with DPG. Taking all these values together and comparing them after normalization to the number of residues (Table 1, last column), the two cases both point into the direction of increased strength of binding. The contribution of bridging waters may be somewhat larger with Cl^- and smaller with DPG. A more significant role emerges in the case of H-

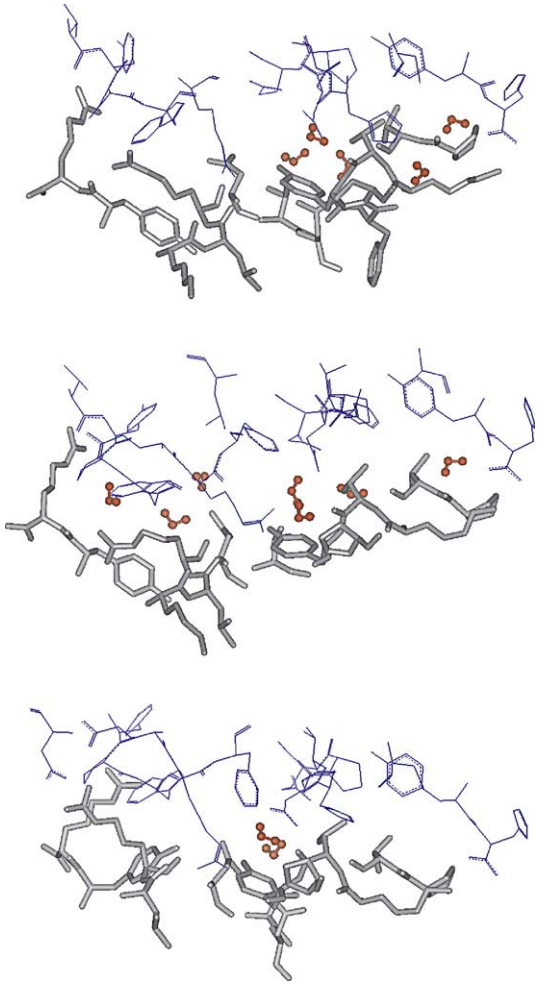

Fig. 2. Comparison of the $\alpha_1\beta_2$ interface in T-state HbA: stripped (top), with DPG (middle), and with chloride bound (bottom) obtained from the 2 ns-average structures. The α_1 residues are rendered blue and the β_2 residues dark grey. Bridging water molecules in the interface gap rendered as red ball and sticks.

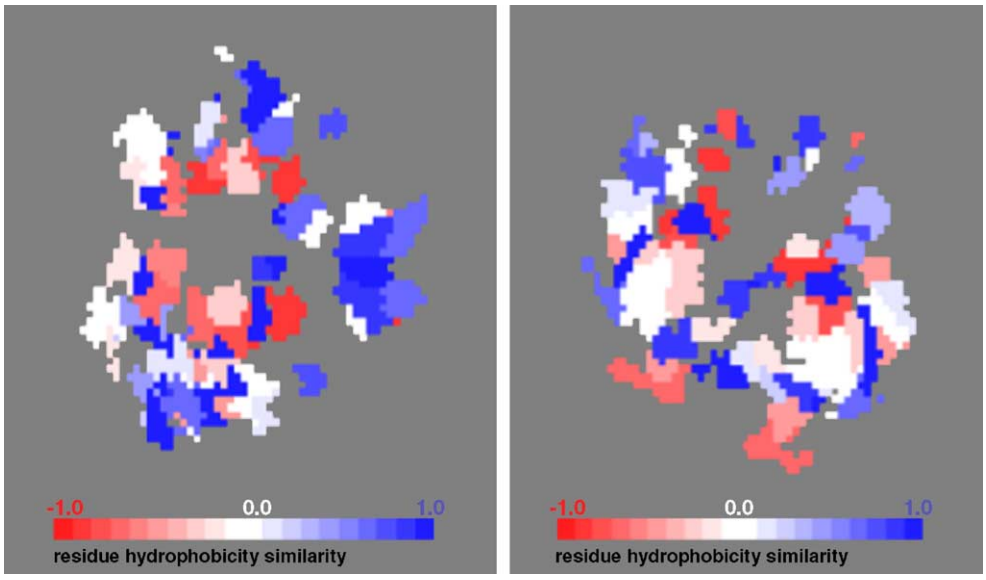

Fig. 3. MolSurfer screen snapshots of the distributions of residue hydrophobicity displayed on 2D maps for the cumulative interdimeric interface region of R-state Hb. Left: stripped R-Hb; right: R-Hb+DPG. The maps are color-coded with dark blue indicating strong hydrophobicity and red strong hydrophilicity.

bonds, showing that their occurrence increases in the following order: stripped < Cl^- < DPG.

The MolSurfer contact maps shown in Fig. 3 detail the distribution of residue hydrophobicity, drastically altered as a result of DPG binding. We consider this as an indication that the contribution of hydrophobic interactions is also increased due to DPG binding, since the hydrophobicity is more uniformly distributed in this case (right side).

3.2. The T state interfaces

In the T state, we evaluate the data also after relating the quantities to the number of residues. After this normalization, the striking effect of binding effectors is the significant increase in the gap volume in the order of stripped < Cl^- < DPG. This effect agrees very well with the experimentally observed K_d increase in the same order which signals a loosening of interface contacts. The same effect is seen in the number of water molecules present in the interface gap. If one compares the gap volume of the stripped R and T states, these data clearly show the tight structure of the T state. This tight binding becomes looser as a result of binding effectors and reaches the condition of the R state when DPG is bound. We note that the parameters of the $\beta_1\beta_2$ interface have contribution only when DPG is bound. This corresponds to the fact that in the T state the central cavity is large and thus no residues form an interface; only when DPG binds, do some residues come closer.

The MolSurfer contact maps in Fig. 4 show that residue hydrophobicity clearly predominates in the stripped case (left

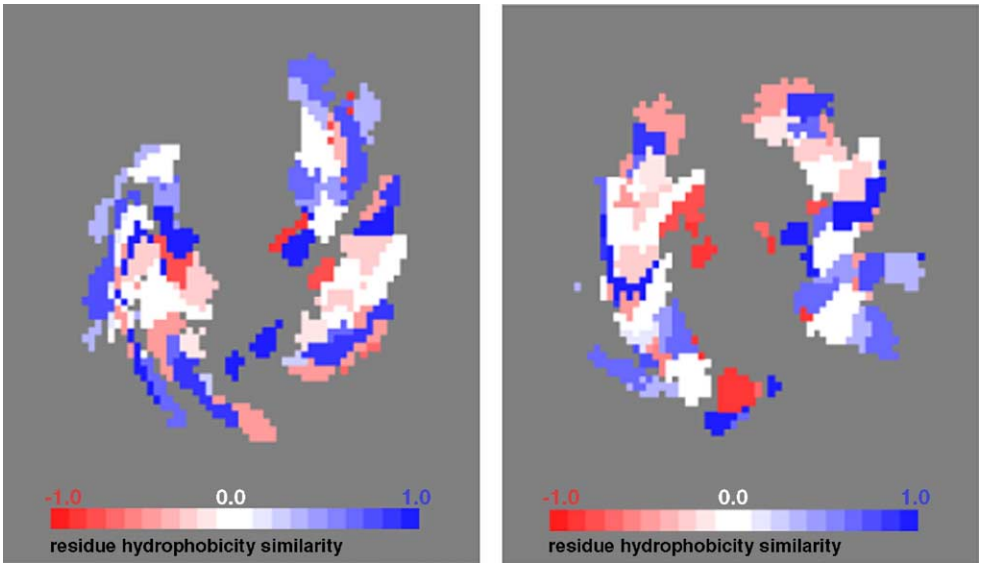

Fig. 4. MolSurfer screen snapshots of the distributions of residue hydrophobicity displayed on 2D maps for the cumulative interdimeric interface region of T-state Hb. Left: stripped T-Hb; right: T-Hb+DPG.

side), indicative of decreased strength of interaction as a result of effector binding (right side).

4. Discussion

The most important message of the computational result is that the average structures extracted from 2 ns MD simulations yield interdimeric interfaces with properties significantly different as a result of significant rearrangements induced by binding effectors. In this paper, we show some features of this rearrangements in Figs. 1–4. For example, it is seen in Fig. 3 that the extent of hydrophilic (red) and hydrophobic (blue) interactions occur as large patches in the stripped case and become more evenly distributed in the DPG-bound case of the R state.

We discuss the overall interface characteristics summarized in Table 1. They support the experimental data shown in Table 2, discussed in detail elsewhere [2]. The experimental data are the dissociation constants for the tetramer–dimer transition at atmospheric pressure and characteristic pressure values (P 1/2) for 50% dissociation. Lower K_d values (and higher P 1/2 values) are indicative of a higher binding energy at the interdimeric interface. The determined dissociation constants agree well with a previous report [15], where tetramer-to-dimer dissociation constants were measured for stripped oxyHb, and also for IHP-bound Hb. A dissociation constant of 1 μM was reported for the stripped case, which decreased to 0.18 μM when bound to IHP. These results are in excellent correlation with our experimental results. A Bohr effect study [16] also reports a value of 0.5–7.9 μM for oxyHb depending on the pH and protein concentration. This again supports our experimental data, showing that dissociation constants determined by the pressure perturbation method yield identical results to data determined by conventional methods. Lower dissociation constants in the R state are indicative of a reorganization of the interfaces upon binding effectors with increased interaction strength between dimers. In the case of the α-oxyFe–β–ZnHb samples (T-state) we observed an overall opposite effect, i.e., an increased dissociation constant upon effector binding, pointing to a decreased interaction strength between dimers.

The structural data extracted from the modeling show that in the **R state**, under stripped condition, the large volume, the high water content and few H-bonds are indicative of loose binding of Hb dimers relative to the T state—as expected. This loose interface becomes tighter with Cl^- binding because the structural rearrangements lead to an increased number of bridging waters and H-bonding. The effect of DPG is characterized by an even larger increase in H-bonding, while the number of bridging waters is less than in the stripped case. The gap volume and the SASA do not change significantly indicating that the overall loose structure relative to that in the T state is not changed dramatically. The binding of effectors to the R state can then be seen as a small perturbation of the properties in the direction of tighter contacts at the dimer interface. This is in agreement with the experimentally observed decrease in the dissociation constant (Table 2). In the case of DPG, decreased H-bonding occurs in the $\beta_1\beta_2$ interface. We believe that this is not indicative of less interaction in this interface, but rather of DPG bridging interface interactions since it has been proposed to bind between these two subunits [6].

In the **T-state**, we observe an opposite trend, namely a decrease in the stabilizing effects (cf. Table 1) shown most conclusively by the increased gap volume. This increase correlates with the increase of the number of interface water molecules. This trend perfectly agrees with the trend shown by the experimental K_d values. Also, the contact maps show a decreased region of interaction in the cumulative interdimeric interfaces as shown for DPG in Fig. 4. All these effects point to the same conclusion, and in the same order, whether based on the modeling results or experimental data.

Considering the K_d values, we find that the strengthening of the dimer interface contact in the R state by effectors is much less pronounced than the loosening effect on the T state (factor of 3 vs. 30). This is due to the interface being already loosely bound in the R state, thus any additional effect is necessarily less pronounced. The larger number of water molecules present in the R-state interface may also shield the effect of overall interface structural reorganization.

Table 2
Experimentally determined K_d and characteristic pressure values of Hb samples [2]

	Effector	K_d (10^{-6} M)	P 1/2 (MPa)
oxyHb	stripped	1.41	100
	100 mM Cl^-	1.22	137
	2 mM IHP	0.47	144
α-oxyFe-β-ZnHb	stripped	0.44	140
	100 mM Cl^-	0.78	113
	2 mM DPG	2.06	95
	2 mM IHP	12.9	72

5. Conclusions

Based on our results, the following conclusions can be derived concerning the structural features behind the experimentally observed effect of binding allosteric effectors on the dimer interface of HbA.

(1) The intrinsic fluorescence of the Trp residues in HbA recorded as a function of increasing hydrostatic pressure yields K_d dissociation constants of the tetramer-to-dimer transition at atmospheric pressure (2). These values are indicative of changes of tetrameric stability upon binding allosteric effectors both in the R and in the T state.
(2) The K_d values show decreased stability in the T state and increased stability in the R state as result of effector binding;
(3) The analysis of interface properties performed on the MD models (number of interface residues, hydrogen bonds, interface water molecules, gap volume, SASA) was used to unravel the structural basis of the experimentally observed changes in the K_d values. In the R state, the association of the dimers is strengthened by increased H-bonding and bridging water molecules as a result of binding allosteric effectors. In the T state, the gap volume

increases and incorporates more water molecules when effectors are bound. The parameters in the case of DPG-bound T state HbA are similar to that in the R state under stripped condition.

(4) Both sets of data are indicative of significant reorganizations occurring at the interdimeric interface region upon binding effectors. Figs. 1–4 show details of these reorganizations and show that this is a significant effect. Thus, we conclude that the changes in the Hb dissociation constant as a result of effector binding can be viewed as a consequence of structural changes propagating from the effector binding site(s) to the interfaces (experimentally monitored by interface-Trp fluorescence). If structural changes occur at the interface, they necessarily must be of a tertiary nature. In this view, the main mechanism of effector action is then to modify the tertiary structure of the subunits, as stated in the global allostery model. This effect is found in both the R and the T states of HbA.

Acknowledgements

Financial support is acknowledged from the Fogarty International Center (Award #TW005924-TY-JF), from NIH grant HL 14508 (TY), by Hungarian grants OTKA TS-044730/2002 (JF), ETT SO1/2003 (JF) and European Union D30 COST action (JF), as well as from the Richter Gedeon Centennial Foundation (PhD fellowship, IK).

References

[1] J. Baldwin, C. Chothia, Hemoglobin: the structural changes related to ligand binding and its allosteric mechanism, J. Mol. Biol. 129 (1979) 175–220.
[2] G. Schay, L. Smeller, A. Tsuneshige, T. Yonetani, J. Fidy, Allosteric effectors influence the tetramer stability of both R and T states of hemoglobin, J. Biol. Chem. (2005) Submitted.
[3] K. Imai, Allosteric Effects In Hemoglobin, Cambridge Univ. Press, 1982.
[4] T. Yonetani, S.I. Park, A. Tsuneshige, K. Imai, K. Kanaori, Global allostery model of hemoglobin. Modulation of O(2) affinity, cooperativity, and Bohr effect by heterotropic allosteric effectors, J. Biol. Chem. 277 (2002) 34508–34520.
[5] A. Tsuneshige, S. Park, T. Yonetani, Heterotropic effectors control the hemoglobin function by interacting with its T and R states—A new view on the principle of allostery, Biophys. Chem. 98 (2002) 49–63.
[6] M. Laberge, I. Kövesi, T. Yonetani, J. Fidy, R-state hemoglobin bound to heterotropic effectors: models of DPG, IHP and RSR13 binding sites, FEBS Lett. 579 (2005) 627–632.
[7] B.R. Brooks III, R.E. Bruccoleri, B.D. Olafson, D.J. States, S. Swaminathan, M. Karplus, CHARMM: a program for macromolecular energy, minimization and dynamics calculations, J. Comp. Chem. 4 (1983) 187–217.
[8] M. Nelson, W. Humphrey, A. Gursoy, A. Dalke, L. Kalè, R.D. Skeel, K. Schulten, NAMD-A parallel, object-oriented molecular dynamics program, Appl. High Perform. Comput. 10 (1996) 251–268.
[9] M.F. Colombo, D.C. Rau, V.A. Parsegian, Reevaluation of chloride's regulation of hemoglobin oxygen uptake: the neglected contribution of protein hydration in allosterism, Proc. Natl. Acad. Sci. U. S. A. 91 (1994) 10517–10520.
[10] U. Essmann, L. Perera, M.L. Berkowitz, T. Darden, H. Lee, L.G. Pedersen, A smooth particle mesh Ewald method, J. Chem. Phys. 103 (1995) 8577–8593.
[11] R.A. Laskowski, SURFNET: a program for visualizing molecular surfaces, cavities and intermolecular interactions, J. Mol. Graph. 13 (1995) 323–330.
[12] M.L. Connolly, Solvent-accessible surfaces of proteins and nucleic acids, Science 221 (1983) 709–713.
[13] R.R. Gabdoulline, R.C. Wade, D. Walther, MolSurfer: a macromolecular interface navigator, Nucleic Acids Res. 31 (2003) 3349–3351.
[14] D. Eisenberg, R.M. Weiss, T.C. Terwilliger, W. Wilcox, Hydrophobic moments and protein structure, Faraday Symp. Chem. Soc. 17 (1982) 109–120.
[15] S. White, Titration of the carboxyhemoglobin tetramer–dimer equilibrium by inositol hexaphosphate, J. Biol. Chem. 251 (1976) 4763–4769.
[16] D.H. Atha, A. Riggs, Tetramer–dimer dissociation in hemoglobin and the Bohr effect, J. Bol. Chem. 251 (1976) 5537–5543.